Fate of the initial state perturbations in heavy ion collisions. II. Glauber fluctuations and sounds

Pilar Staig and Edward Shuryak
Department of Physics and Astronomy, State University of New York, Stony Brook, New York 11794, USA
(Received 22 June 2011; revised manuscript received 5 August 2011; published 20 September 2011)

Heavy-ion collisions at the BNL Relativistic Heavy Ion Collider (RHIC) are well described by the (nearly ideal) hydrodynamics for average events. In the present paper we study initial state fluctuations appearing on an event-by-event basis and the propagation of perturbations induced by them. We found that (i) fluctuations of several of the lowest harmonics have comparable magnitudes and (ii) that at least all odd harmonics are correlated in phase, (iii) thus indicating the local nature of fluctuations. We argue that such local perturbations should be the source of the "tiny bang," a pulse of sound propagating from it. We identify its two fundamental scales as (i) the "sound horizon" (analogous to the absolute ruler in cosmic microwave background and galaxy distributions) and (ii) the "viscous horizon" separating damped and undamped harmonics. We then qualitatively describe how one can determine them from the data and thus determine two fundamental parameters of the matter: the (average) speed of sound and viscosity. The rest of the paper explains how one can study mutual coherence of various harmonics. For that, one should go beyond the two-particle correlations to three (or more) particles. Mutual coherence is important for the picture of propagating sound waves.

DOI: 10.1103/PhysRevC.84.034908 PACS number(s): 25.75.Ld, 25.75.Gz, 12.38.Mh

I. INTRODUCTION

Starting the introduction, let us note that the issues to be discussed in this paper are somewhat similar in nature to current trends in cosmology of the last decade, which made it a really quantitative science. The sound horizon scale has been seen on the sky, in correlations of cosmic microwave background temperatures, and in locations of the galaxies.

Experimental data obtained in heavy-ion collisions at the BNL Relativistic Heavy Ion Collider (RHIC) have found the "little bang," a hydrodynamical explosion driven mostly by pressure of the new form of matter, the quark-gluon plasma (QGP). Their experimental data for radial and elliptic flows have been compiled in the so-called "white papers" of RHIC experiments [1–4] in 2004 and compared with predictions of relativistic hydrodynamics. The models which implemented freezeout via hadronic cascades [5–7], as originally suggested in [8], were found to be especially successful. Very recent results from the Large Hadron Collider (LHC) on elliptic flow [9] also turned out to be in agreement with hydrodynamical predictions, suggesting that the QGP remains a good liquid even at LHC (see, e.g., Ref. [10]). Dissipative effects from the QGP viscosity provide only small corrections at the few-percent level; see [11–13]. So, by now, we have quantitative overall description of the "little bang."

This paper is about small deviations from this average behavior. Such perturbations of the average explosion can come from at least two different sources. The one which we will study in this paper is due to quantum fluctuations in the wave function of the colliding nuclei, which creates "bumpy" distributions of matter, for any collision, which one can decompose into a smooth average plus local perturbations.

The smallness of the perturbation amplitude, with respect to the local density of ambient matter, would suggest the appearance of divergent sound waves; see Fig. 1. Similar to the circles from a stone thrown into a pond, hydrodynamics tells us that initial perturbations should become moving waves, with basically nothing left at the original location at later time. This is the picture we are going to work on in this paper.

Another one, to be studied in subsequent papers of this series, are created by the energy deposited by jets propagating through the medium. It has been recently dramatically shown by the ATLAS Collaboration [14] that even jets with energy above 100 GeV deposit a large part of their energy, and sometimes all of it, into the medium. The first ideas were to look at the resulting perturbations in the form of a Mach cone [15], driven by the view that the energy is deposited more or less homogenously along the jet path. However, more recent developments of the theory, based on anti–de Sitter-space/conformal-field-theory (AdS/CFT), have lead to the view that the deposited energy grows rapidly with the distance traveled by the jet, with significant deposition at the end point. Thus, one may think of the second kind of "tiny bangs," this time occurring in between the beginning and the end of the "little bang." Obviously those should lead to sound circles of smaller absolute and angular sizes.

An alternative idea of randomly fluctuating shapes of the initially produced fireballs has resulted in an approach in which different angular harmonics of that distribution are treated separately. The realization that even central $\vec{b} = 0$ collisions may have some fluctuating ellipticity has led to the discussion of elliptic flow event-by-event fluctuations; see Ref. [16] and many subsequent works. The so-called triangular flow related to the fluctuations in the third harmonic of the flow has been recently studied in an important paper by Alver and Roland [17], with many groups working in this direction now.

The main difference between our approach and that is that we treat such fluctuations not as independent (Gaussian) noise in different harmonics but as certain local perturbations, resulting in certain evolving sound fronts that reach a certain size, shape, and diffusivity by the moment of freezeout. In other words, we think that various harmonics are mutually coherent. One of the main goals of this paper is to explain how this

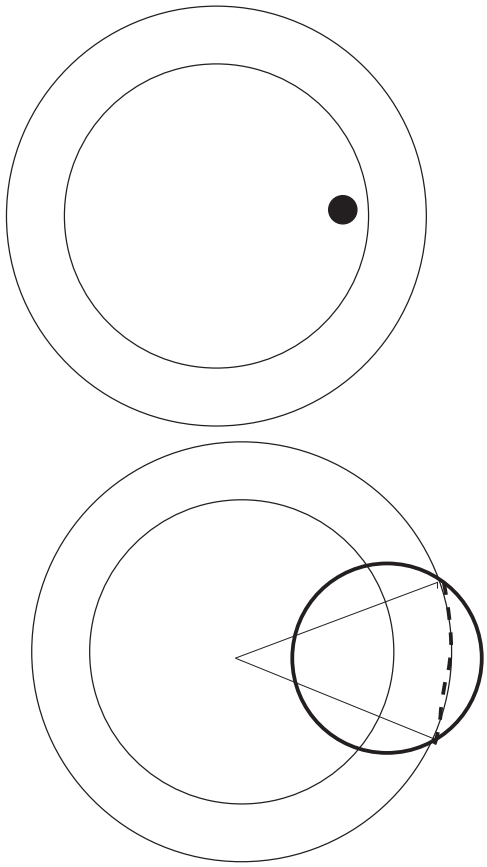

FIG. 1. Sketch of the transverse plane of the colliding system: the two concentric circles are the nuclear radius (inner) and the final radius of the fireball (outer). The black spot in the upper figure is an extra density due to initial density fluctuations. The small perturbation becomes a circle of a sound wave, which will be stopped at freezeout at the thick circle (distorted by radial flow). The part outside the fireball does not exist: the corresponding matter will actually be placed near the edge of the fireball (thick dashed line). The angle between the two thin lines corresponds to the angle between two peaks in the resulting angular distribution.

coherence can be tested experimentally. We will also provide evidence (based on the Glauber model of the perturbations) that such mutual coherence is present in this model.

(On one hand, one may argue that, as soon as all the perturbations are small and the equations are linear, it is not important if one expands in harmonics before or after the solution of hydro equations. So the solution to hydro that we will discuss in our next companion paper [18] can be used for both "noise" and coherent scenarios.)

Let us also briefly recall the history of the theoretical efforts. The propagation of sound on top of the fireball has been discussed by J. Casalderrey-Solana and one of us in Ref. [19]. In that paper the fireball expansion was modelled by the big-bang-like overall expansion of the space, with the same Friedman-Robertson-Walker metric as used for cosmology. The focus of that paper was the effect of time-dependent sound velocity, especially if the phase transition is first order and can vanish at some interval of T. The interesting finding was the creation of the secondary—and convergent—sound waves. This idea was further discussed in [20] in connection with the "soft ridge" issue, but with the conclusion that, if the current lattice data on the speed of sound is correct, the effect of the reflected wave is too small.

In the same paper [20] it has been found that the usual (unreflected) sound propagation should produce characteristic "two-peak events," with the angle between the peaks reflecting the sound horizon and numerically being about 1 radian. More specifically, this angle corresponds to the angle at which two intersections of the fireball boundary are seen from the fireball center. The Brazilian group [21] has independently found such peaks with the same angle, induced by a local perturbation. Andrade *et al.* have further pointed out that the two-peak events lead to a three-peak correlation function, with the side peaks separated by twice the larger angle $\sim$2 rad. This observation explained what has been found earlier, in the average over many events, in "event-by-event" hydrodynamical studies by the Brazilian group (see Ref. [22] and references therein) and Werner *et al.* [23]. Good agreement between the shapes of the correlation function in "event-by-event" pictures and single local perturbation indicate that the former are more or less linear superpositions of the latter ones.

Completing this introduction, let us note that this paper was completed and submitted to archive in August 2010, but it was submitted to Physical Review C in June 2011 together with its companion paper [18]. During this time there were obviously many papers devoted to the subject. In particular, Glauber model predictions for several harmonics ϵ_n and their root-mean-square fluctuations have been calculated independently several times. The Qin *et al.* [24] paper is an example, which also considered the influence of inelasticity fluctuations of the $p+p$ reaction on the initial density fluctuations. Significant experimental progress resulted now in measurements of higher harmonics to $n=9$, by all five collaborations at RHIC and LHC. Yet the main suggestion of this work—the measurements of the mutual phases of those harmonics—still remains to be done in the future.

II. SETTING UP THE PROBLEM

A. Main scales of the problem

Before going to specifics, let us formulate the problem in a more general form. Two generic scales of the hydro approach are (i) the macroscopic scale R and the microscopic scale l, being in the relation

$$l \ll R, \tag{2.1}$$

which ensures that macroscopic tools such as thermodynamics and hydrodynamics should work.

Now let us define two new scales. The first is the sound horizon

$$H_s = \int_{\tau_i}^{\tau_f} d\tau c_s(\tau), \tag{2.2}$$

where the integral is taken from the formation of the hydro system to its freezeout time. While in the big bang $\tau_f \sim$ 100 000 years, in the little bang it is only $\sim$10 fm. It is important that in both cases, at the freezeout, the collisions

cannot support pressure any more, yet the sound wave does not disappear—it just stops—and thus it can be observed. For the big bang this idea was suggested by Sunyaev and Zeldovich 30 years ago [25], who dubbed the sound horizon the "standard ruler" of the universe. Its current value, $H_s \approx 150$ Mps, as seen in the galaxy's distribution and in the Cosmic Microwave Background (CMB) radiation correlations, is an excellent way to measure the Hubble constant and the lifetime of the universe.

In the cosmology such scale corresponds to angles of about 1 degree and thus $l \sim 200$. In the little bang, we deal with about 1 radian and $m \sim 3$.

The second scale (not important in cosmology), which we would like to call "the viscous horizon scale" R_v, separates the wavelengths of the sound which are and are not dissipated by the viscosity effects. The smooth fireball and fluctuations are described by

$$T_{\mu\nu} = \tilde{T}_{\mu\nu} + \delta T_{\mu\nu}. \tag{2.3}$$

The textbook dispersion law for the sound, including the viscosity term, is

$$\omega = c_s k - \frac{i}{2}\frac{4\eta}{3s}\frac{k^2}{T}. \tag{2.4}$$

A Fourier transform puts it into momentum form, after which one can solve the time dependence using the momentum-dependent dispersion relation as well as the imaginary part induced by viscosity.

One may add bulk viscosity to this expression as well, but we keep the shear viscosity for now, assuming it is dominant:

$$\delta T_{\mu\nu}(t) = e^{-\frac{2}{3}\frac{\eta}{s}\frac{k^2 t}{T} + ik(x - tc_s)}\delta T_{\mu\nu}(0). \tag{2.5}$$

The first term in the exponent defines the new viscous survival scale: harmonics with $k \ll k_v$ would be little affected and, with $k \gg k_v$, they would be killed. The definition of this scale is clear from the exponent

$$k_v = \frac{1}{R_v} = \sqrt{\frac{3Ts}{2\tau_f \eta}}. \tag{2.6}$$

While the sound horizon determines the size of the sound circles at freezeout, the viscous one determines their width. Note that, while the former increases linearly with time $H_s \sim t$, this width $R_v \sim \sqrt{t}$. So, although the spheres become more diffuse, they are also relatively sharper as time goes by.

One may also ask the very good question of how the early hydrodynamical description of the perturbations may be valid. We will not go into its discussion here but only state that the applicability limits of Navier-Stokes hydrodynamics is not determined by the k_v scale, but by the magnitude of the higher-order terms in gradients, resummed. The last word is added because of the issue of alternating sign of the series, which is raised in the "universal resummed hydrodynamics" paper [26]. For the last works on the subject in the AdS/CFT context see, for example, Ref. [27], in which the convergence of a large class of nonequilibrium evolutions to such universal behavior is indeed demonstrated and its applicability limits are discussed quantitatively.

How can one experimentally measure the two scales, H_s and $1/k_v$, which define the speed of sound and viscosity? One may change the geometry of the collision (by centrality) and the size of the nucleus (by changing beam A), but an even better way is by observing many angular harmonics of the flow. Note that the amplitudes of the higher harmonics are more damped by viscosity so, if measured, they would provide a measure of the viscosity.

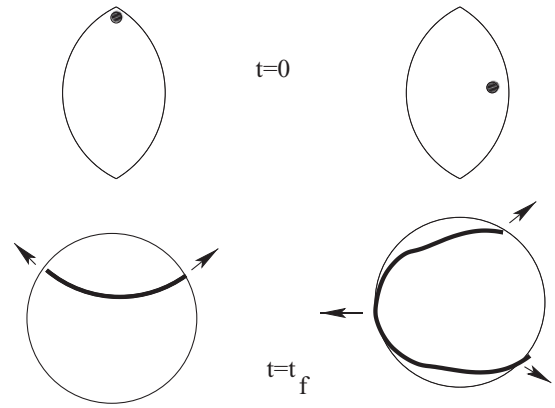

FIG. 2. The two upper pictures correspond to initial time $t = 0$: the system has an almond shape and contains perturbations (black spots). The two lower pictures schematically show location and diffuseness of the sound fronts at the freezeout time t_f. The arrows indicate the angular direction of the maxima in the angular distributions 2 and 3, respectively.

For central collisions at RHIC-LHC, the hierarchy relation between all four of these scales is

$$R \sim H_s > R_v > l. \tag{2.7}$$

As some representative numbers, let us mention 8, 6, 1, 1 fm (at freezeout), respectively. However for mid-central collisions the width (the shorter size) of the "almond" R_x becomes comparable to or smaller than H_s. As a result, one expects the sound wave to traverse the whole fireball and deposit some amount of (entropy) density at its opposite side. In this case one expects three-peak events; see Fig. 2 for explanation. So, one of our suggestions to experimentalists is to study the centrality at which certain changes in harmonics amplitudes and phases may occur.

III. INITIAL STATE FLUCTUATIONS

A. Generalities

Let us start with a comment on what we would call the "initial state." This term is currently used in at least three different settings: (i) The setting of the wave function of the colliding nuclei, expressed either in terms of the nucleons (their positions in the transverse plane just prior to the collisions) or in terms of partonic degrees of freedom (positions and longitudinal momenta). Another version is the "color glass condensate" (CGC), which is described as an ensemble of classical gauge fields. (ii) The state just after the (Lorentz contracted) nuclei passed each other. It is either the partonic state, including partons newly produced in a collision, or the so-called glasma, in the classical field description. (iii) The setting of the state after approximate equilibration is reached,

so that the macroscopic (hydrodynamical) description can be started.

It is the last setting which we mean in this work, as we would apply hydrodynamics as a tool, translating properties of the initial conditions into the final state observed in the experiment. Therefore our "initial state" should correspond to about one unit of the relaxation time after the actual collision, or numerically to a proper time of the order of $1/2$ fm/c. Thus the inhomogeneity of the initial wave functions should already be smoother than at time zero, by this (so far poorly understood) relaxation process.

As we detail below, this state will be described by some "average" or zeroth-order shape of the fireball (depending of course on the impact parameter, the colliding nucleus, and the collision energy), plus "fluctuations" characterized in first order by an ensemble of small perturbations of the average shape described by Fourier coefficients and phases $\{\epsilon_n, \psi_n\}$. Generic expressions would include the zeroth-order ensemble-average deformations $\langle\epsilon_n\rangle$ and deviations which have no average but fluctuations $\delta\epsilon_n^2 = \langle\epsilon_n^2\rangle - \langle\epsilon_n\rangle^2$.

The simplest situation, which happens for the second harmonics and sufficiently peripheral collisions, is that the average is much larger than the fluctuations: $\langle\epsilon_2\rangle \gg \delta\epsilon_2$. If so, one may assume a Gaussian form of the fluctuations with the width given by $\delta\epsilon_2$. But in general the situation is quite different; the odd harmonics are always due to fluctuations and also, for near-central collisions, for all n both terms in ϵ_n come from fluctuations. Until $n < 10$ they are comparable in magnitude $\epsilon_n \sim 1/10$ with wide fluctuations. (The distributions are obviously non-Gaussian because they are all positive by definition.) All of those should in principle be provided by some "initial state models," of which we select the Glauber model as the simplest example.

The separation of the initial state fluctuations from all other fluctuations (e.g., fluctuations during the hydrodynamical evolution, hadronization, and the freezeout) is possible because of the fundamentally different number of relevant degrees of freedom defining their magnitude. As we will detail in the next section, the so-called Glauber fluctuations due to various number of "wounded" (or participant or interacting) nucleons are of the order of

$$\epsilon_n \sim \frac{1}{\sqrt{N_p}}, \tag{3.1}$$

where the number of the participant nucleons $N_p \sim O(100)$, being limited from above by the total nucleon number $2A \sim 400$.

Further fluctuations are determined similarly, but with the number of participants N_p substituted by the much larger number of partons involved, or the total multiplicity $N_{\text{hadrons}} \sim 10^4$ (for RHIC and LHC it is a factor of 2 different). That is why one may, to a certain accuracy, ignore all later-time fluctuations and assume that observable fluctuations in particle spectra and correlation functions are one-to-one translated from the initial state ensemble. Thus we use hydrodynamical equations as a fully deterministic tool, by itself producing no random numbers at all.

Furthermore, for near-central collisions all $\delta\epsilon_n$ are small, of the order of several percent. So, independently of their possibly complicated distributions and cross correlations, the hydrodynamics applied in linear approximation should be a quite reliable tool. Thus hydro equations can be linearized and the linear response coefficients $\delta v_n/\delta\epsilon_n$ can be calculated. If so, it does not matter what the actual magnitude of the deformation $\delta\epsilon_n$ is. Also, the linearized perturbations do not interact with each other.

Although we will focus on these calculations in our next paper, let us note here two things: One simple fact is that, while angles ψ_n of the fireball deformations indicate the maxima of the distribution (the corners of triangle, square, and other polygons), hydro flow goes along their sides. Therefore, the observed flow angles ξ_n are rotated from the deformation angle as follows:

$$\xi_n = \psi_n + \frac{\pi}{n}. \tag{3.2}$$

Our second comment is that higher harmonics n oscillate with time, displaying acoustic sound properties. At freezeout this leads to their certain signs, and these phases should be added to this relation as well.

B. Fluctuations in Glauber model: the amplitudes

Our "Glauber model" is a bit different from that used widely by experimentalists. Both assume that initial state fluctuations originate from the nuclear wave functions. The "usual Glauber" uses randomly placed coordinates of the individual nucleons in the nuclear wave function. However, the nucleons themselves are complicated objects and their interactions are also strongly fluctuating. Since there are studies of that we decided to also include this source of fluctuations. This changes the numbers a bit, but is found not to be important for any of the qualitative conclusions to be reached.

The nucleon fluctuations we included via the fluctuating NN cross sections are, to a certain degree, known and studied via diffraction, see [28] for the details and earlier references. Naively, from the well-known fact of a nucleon being made of quite a large number of partons one might conclude that those fluctuations are small $[O(1/N_{\text{partons}})]$, but this is not the case. In our simulation we assumed the cross section σ_{NN} to be the random Gaussian variable with the variance

$$w_{NN} = \frac{\langle\sigma_{NN}^2\rangle - \langle\sigma_{NN}\rangle^2}{\langle\sigma_{NN}\rangle^2} \approx 0.25. \tag{3.3}$$

First, like in [17], we simulate a large ensemble of collisions and calculate the magnitude of the ϵ_n for several of the lowest harmonics (up to 6). Their definition is via the Fourier expansion for a single-particle distribution:

$$f(\phi) = \frac{1}{2\pi}\left(1 + 2\sum_n \epsilon_n \cos[n(\phi - \psi_n)]\right), \tag{3.4}$$

where the ϵ_n are the participant anisotropies and the ψ_n are the angles between the x axis and the major axis of the participant distribution.

The participant anisotropies are calculated from

$$\epsilon_n = \frac{\sqrt{\langle r^n \cos(n\phi)\rangle^2 + \langle r^n \cos(n\phi)\rangle^2}}{\langle r^n \rangle}. \quad (3.5)$$

This expression is calculated in the center of mass of the participant nucleons for each event. Therefore, the dipole moment $n = 1$ made out of the average coordinates

$$\langle x \rangle = \langle r \cos(\phi)\rangle = 0, \quad \langle y \rangle = \langle r \sin(\phi)\rangle = 0, \quad (3.6)$$

are zero by definition.

The two-dimensional (2D) shape of the event can in principle be expanded in the double Taylor series in x, y or in a double series over the moments $r^m \cos(n\phi)$, $r^m \sin(n\phi)$ with integer m, n. An even better definition would be to follow the customary statistical trick and write the distribution as the exponent containing the "generating function" of the angular dependence expanded in harmonics:

$$P = F_1(r)\exp(F_2), \quad F_2 = \sum_{n>0} r^n \epsilon_n \cos[n(\phi - \psi_n)]. \quad (3.7)$$

In this way the positivity of the distribution function, as well as inclusion of trivial higher-order effects, are ensured.

Since the dipole $m = n = 1$ term is zero by construction, we define the first odd deformation ϵ_1, ψ_1 using the term of the expansion $m = 3$, $n = 1$ which appears together with the triangular deformation $m = n = 3$:

$$\epsilon_1 = \frac{\sqrt{\langle r^3 \cos(\phi)\rangle^2 + \langle r^3 \cos(\phi)\rangle^2}}{\langle r^3 \rangle}. \quad (3.8)$$

The anisotropies calculated in this way are plotted in Fig. 3 for $n = 1,\ 6$. The plot shows that the eccentricity has the largest value for the well-known elliptic deformation ϵ_2 and a nonzero value of triangularity ϵ_3, in agreement with the results reported in [17]. Note that, for the near-central collisions $N_{\rm part} > 300$, the elliptic deformation is no longer dominant, and it is also due to fluctuations. This conclusion becomes evident as one looks at the lower plot of Fig. 3 , which shows the variations of these ϵ_n.

One observation coming from these results is that all other deformations (except for ϵ_1, which is small because the "true dipole" remains zero) are all comparable, ranging from $O(1/10)$ for central collisions to 0.3 to 0.5 for most peripheral ones. While in the central bins these perturbations can be considered small and treated as Gaussian random variables, it is clear that, for most peripheral bins (when the number of participants is smaller), the fluctuations are large and thus must be non-Gaussian.

Another consequence is that there is absolutely no ground to single out ϵ_3. In fact, both ϵ_4 and ϵ_5 are larger that ϵ_3, and ϵ_6 is about of the same order as ϵ_3.

The last point is that their variations (the lower plot) are all comparable to the magnitude. Yet the definition of deformations are such that they are always positive, for each event. This is one more reason why the amplitudes cannot have a Gaussian distribution, deviating from it at least for the smallest values.

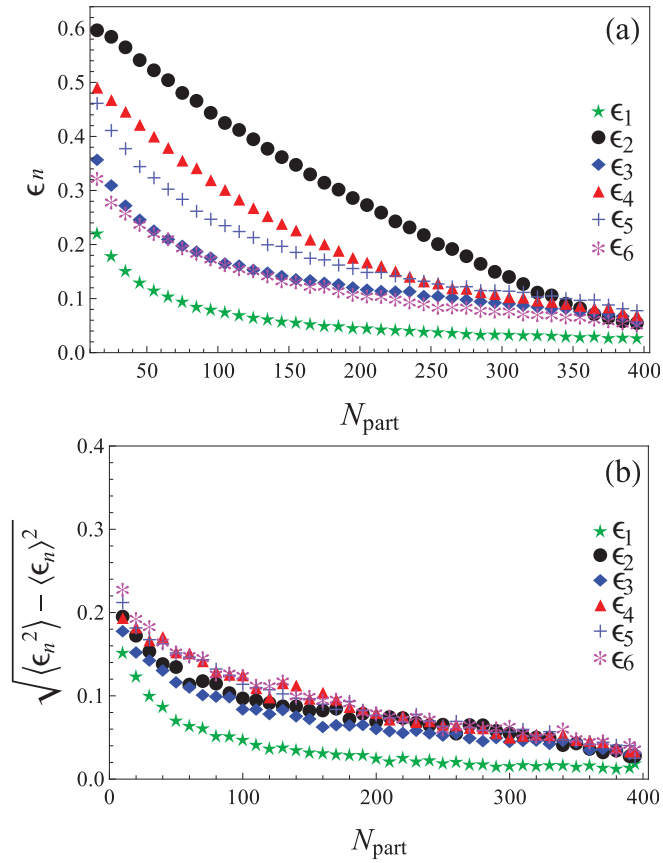

FIG. 3. (Color online) Average anisotropies (a) and their variations (b) as a function of centrality expressed via the number of participants $N_{\rm part}$.

C. Fluctuations in Glauber model: the angles

The angles ψ_n are defined by

$$\tan(n\psi_n) = \frac{\langle r^n \sin(n\phi)\rangle}{\langle r^n \cos(n\phi)\rangle}, \quad (3.9)$$

and to calculate ψ_1 we use

$$\tan(\psi_1) = \frac{\langle r^3 \sin(\phi)\rangle}{\langle r^3 \cos(\phi)\rangle}. \quad (3.10)$$

Using these expressions we obtain the distribution of the ψ_ns for the first six harmonics as shown in Figs. 4 and 5. In order to better understand the behavior of these angles we will now study their correlation.

(Note that our angle definition is different from the one by Alver-Roland [17]: we do not include the extra phase π/n between the flow and deformation directions; see below.)

Let us comment on these distributions, starting from the even ones.

The most obvious one is a distribution of the second (elliptic) harmonic. As seen in Fig. 4 the angle ψ_2 is strongly peaked at $\pi/2$, corresponding to an elongation of the system in the y direction, as of course one expects from the overlap "almond" of two nuclei. The distribution of the fourth angle ψ_4 in Fig. 5 shows peaks at angles 0 and $\pi/2$, but because of the quartic symmetry of the fourth harmonic it simply means that the maxima of the distribution tend to be aligned with the

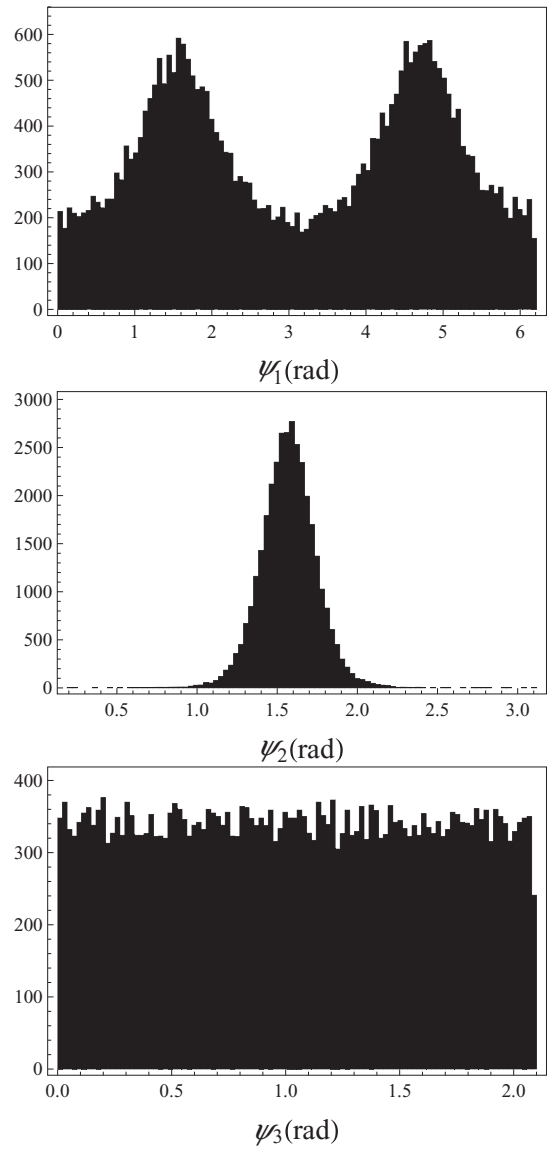

FIG. 4. Distribution of angles ψ_n for first three harmonics. The centrality bin used is $100 < N_{\text{part}} < 300$.

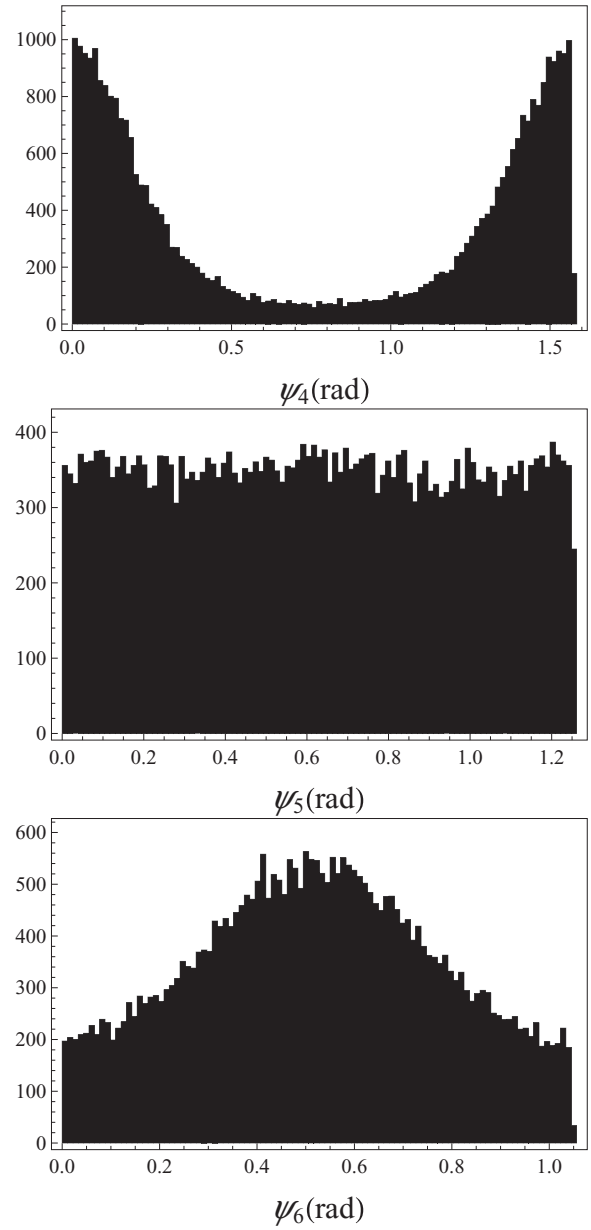

FIG. 5. Distribution of ψ_n for the harmonics 4 to 6. The centrality bin used is $100 < N_{\text{part}} < 300$.

coordinate axes x and y. The distribution of the sixth harmonic is different; it is peaked at the angle $\pi/6$. This means that it has no maximum in the x direction but rather in y. In conclusion, all even harmonics are strongly correlated with the reaction plane, with all of them producing maxima along the y (out-of-plane) direction.

The distribution of the angle ψ_1 is nonzero at all angles, which means it is not very strongly correlated with the reaction plane. It has two maxima, in the $\pm y$ directions, to be called "tip" fluctuations. Although the contribution from angles 0, π, or x directions is about twice smaller, it also makes an important contribution. We will call them "waist" fluctuations. Note that, while the area of the "waist" is larger than that of the "tips," its contribution is smaller.

The distribution over ψ_3, ψ_5 in these figures looks completely uncorrelated with the reaction plane. (This fact has also been noticed in Ref. [17] and by others.) However, further scrutiny shows that they are in fact well correlated with ψ_1; see Fig. 6 (in which we included points repeated by periodicity). The distribution can be crudely characterized by some "bumps" plus "stripes" connecting them.

The interpretation of the "bumps" is that all of them correspond to events with additional "hot spots" at the "tips" of the almond. It is a very natural place for maximal fluctuations, for two reasons: First, this is where the participant density in both nuclei is near zero. Second, because of the factor r^3 they have larger weight than all other places.

There are two kinds of "stripes," those with positive and negative slope in Fig. 6. The latter ones simply follow from the ψ_1 distribution, while the former one is indeed a nontrivial correlation between the angles whose origin we cannot explain. We will continue to discuss its manifestation a bit later. The

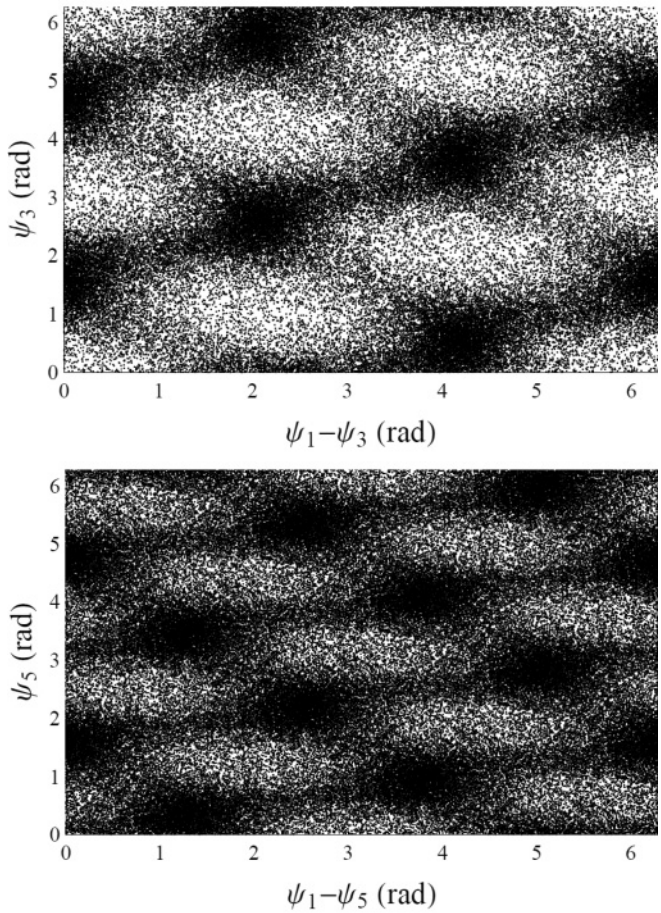

FIG. 6. Scatter plot of the ψ_3 vs $\psi_3 - \psi_1$ (above), and of the ψ_5 vs $\psi_5 - \psi_1$ (below), for $100 < N_{\rm part} < 300$.

correlation of ψ_5 with ψ_1 is very similar. The "bumps" at $\psi_5 - \psi_1 \approx 0$ again mean the $\pm y$ direction or the "tips." The plot has similar "stripes."

Getting a bit ahead of ourselves, let us study the "resonant" combinations of angles as well as angles and amplitudes. As we explain below, those particular combinations of the amplitudes and phases of two harmonics are

$$\left\langle \epsilon_{n_1}\epsilon_{n_2}\cos\left(n_1\psi_{n_1} - n_2\psi_{n_2}\right)\right\rangle, \tag{3.11}$$

especially in the case when n_1, n_2 differ by two units. We have studied two first examples of the kind, with odd harmonics 1, 3, and 5.

One interesting distribution, shown in Fig. 7, is that over the cos term itself for the particular combination of phases 1 to 3. It consists of two clearly different parts: a very narrow peak near -1 and wide flat distributions between -1 and 1. This plot demonstrates a qualitative feature of the phase distribution which was pointed out above. One explanation of the peak near -1 (the angle combination is π) comes from the fluctuations at the "tips" of the almond, when both ψ_1 and ψ_3 are strongly correlated close to $\pi/2$. However, the second interesting correlation seen as "positive slope lines" in Fig. 6(a) because, for them, $\psi_1 - 3\psi_3 = \pi$ as well. A similar situation happens for other odd harmonics.

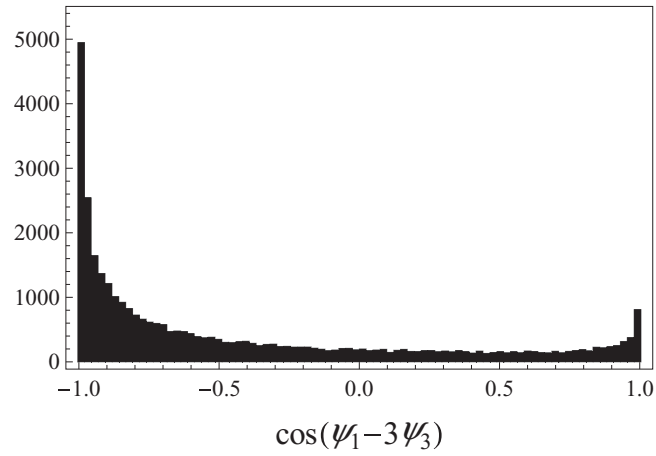

FIG. 7. Scatter plot of $\cos(3\psi_3 - \psi_1)$.

The average value of the combinations (3.11) for harmonics 1 to 3 and 3 to 5 as a function of centrality are shown in Fig. 8. All values are negative, as the sign is dominated by a peak in the cosine near -1: the other component more or less averages out. We thus conclude that experimental measurements of the amplitude of such correlations, with the magnitude and the sign, will be especially sensitive to the "almond tip" fluctuations.

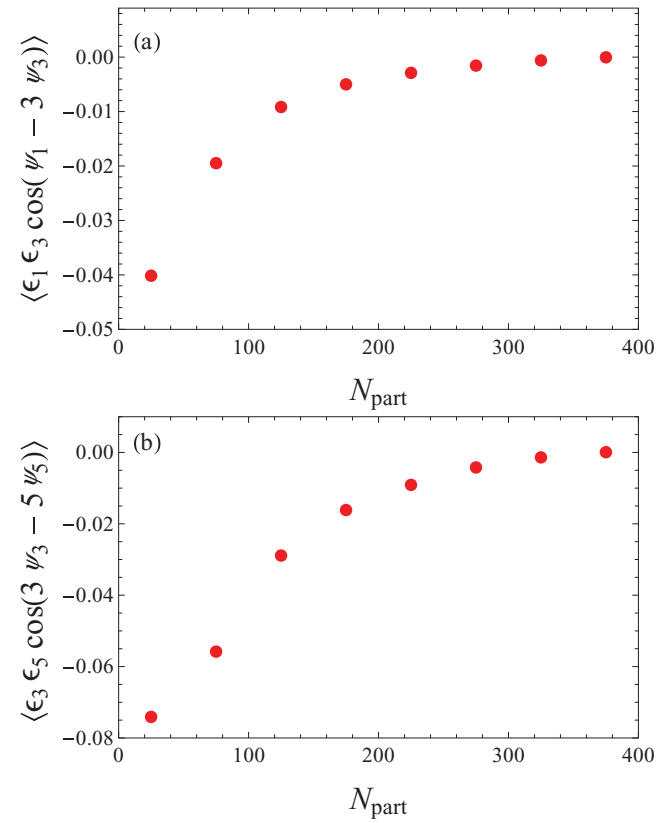

FIG. 8. (Color online) Correlators $\langle\epsilon_1\epsilon_3\cos(\psi_1 - 3\psi_3)\rangle$ (top) and $\langle\epsilon_3\epsilon_5\cos(3\psi_3 - 5\psi_5)\rangle$ (bottom) as a function of the number of participants. The error bars are omitted since they are smaller than the dots.

To summarize the observed pattern, we have found that all odd angles are well correlated with each other, forming the "stripes" and "bumps" shown in Fig. 6. The fluctuations and correlations seem to be stronger from the "tips" of the almond.

D. Comments on other initial state fluctuations

So far the only source of fluctuations included has been (i) the coordinate part of the nuclear wave function prescribing the nucleon positions in the transverse plane and (ii) the event-by-event fluctuations of the NN cross section. We found that the former effect dominates and the latter only provides small corrections.

While other sources of fluctuations clearly are a subject for future studies, we still provide some comments on those.

One important type of "initial state" fluctuation is of course hard parton scattering events, resulting in jet production. The rate of those depend very strongly on the exact definition of the cutoff beyond which the momentum transfer involved is characterized as "hard." There are vastly different opinions on where this boundary is theoretically, and experimentally it depends on whether such events are triggered by single large-p_t hadrons or by some jet-finding algorithms. Jet production and quenching is of course of high interest, but those should be studied only in a small fraction of all collisions selected by separate triggers. For global fluctuations those can safely be ignored, as the probability of "hard" events is smaller than that of the fluctuations we study.

In the Glauber approach that we used, the local density of matter produced is assumed to be simply proportional to the local density of all participant nucleons, $N_p(A_1) + N_p(A_2)$. However, when this density is high enough, it has been argued that the so-called saturation phenomenon should take place, because of parton absorption processes in the wave function. Other expressions for local matter density have been proposed, for example, $\sim \min(N_p) \ln[\max(N_p)/\min(N_p)]$ by Kharzeev *et al.*, where min and max refer to the smaller and the larger of the two, respectively. Those are typically the amplitudes of the fluctuations.

A well-known approach to their description is the so-called glasma, which calculates those color fields from random color charges of the leading (larger x) partons of the two colliding nuclei. Asymptotically (in a very large nuclei or at very high energy) McLerran and Venugopalan [29] argued that, at a particular location in the transverse plane, the color charges of partons must be uncorrelated because they come from different nucleons. Therefore, it is usually assumed that their color charges fluctuate as random variables. If so, the resulting fluctuations are small, as the total number of partons is very large.

The application of such ideas usually keeps the average values of those, such as $A^{1/3}$ or so. The point of our comment is a warning that such simplified ideas cannot be used for determining the fluctuations. It has been known for a long time that, while at very small x, the partons (mostly gluons) become numerous; they are still very tightly correlated in the transverse plane. The size of the "gluonic spot" in the nucleon has been known for a long time from diffractive form factors and, in more recent form, from Hadron-Electron Ring Accelerator (HERA) photon diffraction into J/ψ. This spot is small and therefore bright. As documented, for example, in Ref. [30] (their Fig. 23), the gluon density at the center of the nucleon is about as high as in the center of Ca_{40}. Therefore, a large number of gluons does not yet imply that all of them merge in the transverse plane into a more-or-less homogeneous distribution; the positions of the incoming nucleons still remain the dominant source of the initial state fluctuations.

As the "gluonic spots" from single nucleons remain the source of initial state fluctuations, one may ask if numerous partons coming from it may be correlated in their quantum numbers, forming specific large-amplitude color fields. One particular kind of such field got special attention; namely, the topologically nontrivial gluonic configurations called the QCD sphalerons [31]. They are gluonic field configurations which originate from excitations of the topologically nontrivial vacuum fields (instantons). While they rapidly explode into a multiple gluon state, they strongly violate CP and chiral symmetries locally, producing in particular $\pm 2N_f$ (≈ 6) units of chirality per sphaleron.

As pointed out in Ref. [32], such strong local CP violation induces special event-by-event fluctuations in the CP-odd observables; for example, they should induce charge asymmetry along the magnetic field. Clearly those should be looked at in special studies.

Other coherent color field configurations which deserve to be specially studied are (color-electric) flux tubes. In pp collisions the view that a field created by longitudinally separated charges makes a flux tube is a consequence of confinement, and thus must happen in vacuum. Many popular event generators are based on the Lund model, cleverly parameterizing flux tube production and decay. In AA low-energy collisions many flux tubes are produced, and their possible fluctuations into the so-called color ropes have been studied, initiated by Ref. [33]. If two elementary color charges can be combined, they may either cancel each other or produce higher representations of the SU(3) group, in which case the rope energy (and entropy, after its decay) is proportional to its flux squared. Further applications of these ideas for strangeness production in AA collisions can be found in Ref. [34].

Studies of flux tubes lay dormant until the recent discovery of the so called hard ridge[1] by the STAR Collaboration at RHIC. One possible origin of it [20] is a hydro-carried longitudinal flux tube, created at the hard collision point. This explanation may work provided the flux tubes survive as such until freezeout. As was argued in that paper this indeed should happen at the periphery of the fireball, where matter is not far from the deconfinement transition, forming a kind of "dual corona" of the QGP fireball, similar to a solar corona full of flux tubes.

[1]Note that "hard ridge" should not be confused with "soft ridge." The latter, as discussed in this and other papers, is naturally explained as a combined effect of "harmonic flows" induced by Glauber fluctuations. Hard ridge, associated with the azimuthal direction of the hard trigger particle, does not yet have a widely accepted explanation.

IV. HARMONICS AND THEIR RELATIVE PHASES EXTRACTED FROM CORRELATIONS

A. Central collisions: two- versus many-particle correlators

Let us for simplicity start with idealized central collisions. If the impact parameter is negligible, one may think of the overall system as completely symmetric in the azimuthal angle ϕ.

A particular event has a certain perturbation which breaks this symmetry. Its (two-dimensional) distribution over transverse momenta of the secondaries can be decomposed into a Taylor series of the momenta p_x, p_y or into the angular harmonics

$$\frac{dN}{dp_t^2 d\phi} = f(p_t)\left\{1 + \sum_{n>0}[2a_n \cos(n\phi) + 2b_n \sin(n\phi)]\right\},$$
$$a_n = \langle \cos(n\phi)\rangle, \quad b_n = \langle \sin(n\phi)\rangle. \tag{4.1}$$

Note that, instead of the curly brackets, one can also use the exponent of the sum, which will include trivial higher-order effects and enforces positivity of the distribution. But we would assume all v_n to be very small, for simplicity.

Instead of using the a, b pair, one may also introduce the moduli and the phases, writing them as $2v_n \cos[n(\phi - \xi_n)]$ with positive v_n. In order to simplify subsequent formulas, we however prefer to write it using the complex exponent:

$$\frac{dN}{dp_t^2 d\phi} = f(p_t)\left(\sum_n v_n e^{in\phi - in\xi_n}\right), \tag{4.2}$$

where the sum goes over all integer n, positive and negative, with $v_0 = 1$ and $v_{-n} = v_n$.

Before going any further, let us give an example of such decomposition for shapes we are interested in. We already mentioned that the sound circles from point perturbations lead to a two-maximum distribution, with an angle of about 1 rad. To make the points, we select the angle between the peaks to be exactly $2\pi/3$, put them at certain positions, and give an arbitrary width for plotting convenience. The result is shown in Fig. 9(a) as a (black) solid curve.

We then do the Fourier decomposition and find that, for symmetry reasons, all coefficients of sinusoidal waves are zero: $b_n = 0$. To understand the relative magnitude of the harmonics one can plot the Fourier "power spectrum" of the squares a_n^2 versus n; see Fig. 9(b). (This is the information which is included in the two-particle correlation function; see below.) The first lesson is that "triangular" harmonics 3, 6, 9, . . . of the type $3k$, k integer, are significantly enhanced relative to other ones. The reason for this becomes apparent if one compares the sum of such modes (the red dashed curve) and the rest of harmonics (the blue dash-dotted curve) with the original shape. "Triangular" harmonics get a coherent enhancement from the three-horn distribution they describe, while the main role of the rest of the harmonics is to cancel this nonexisting third horn and nonexisting negative region in between the horns. This interpretation is confirmed by the signs of the harmonics a_n: all "triangular" ones are positive and all others are negative. So, if one would like to reconstruct the distribution from its Fourier series, one may, for example, find the amplitudes from the power spectrum and the relative signs (phases) of the harmonics.

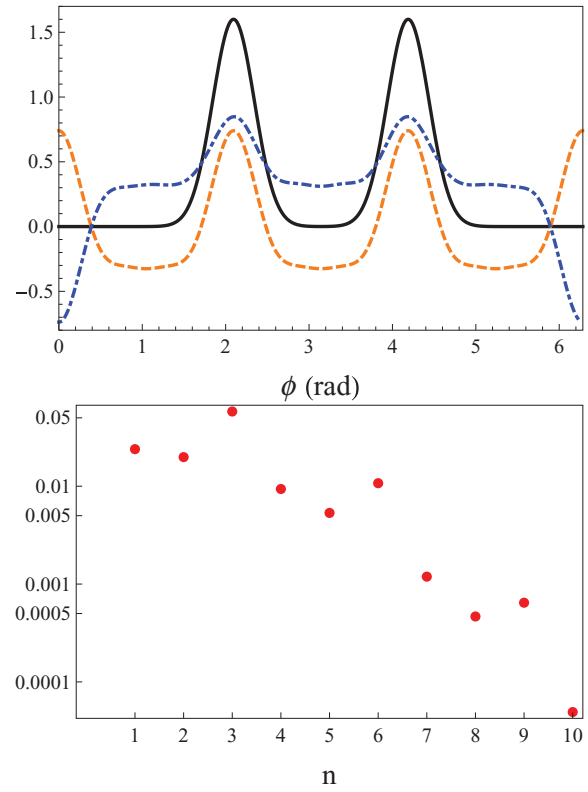

FIG. 9. (Color online) (Upper panel) Two-peaked solid (black) curve is the example of single-particle angular distribution to be discussed. The (red) dashed curve is the sum of the 3, 6, and 9 harmonics, while the (blue) dash-dot curve is the contribution of all other harmonics with $n < 10$. (Lower panel) The corresponding "power spectrum" of the harmonics: a_n^2 versus n.

At the end of Sec. III we suggested that sufficiently peripheral collisions would result in three-peak distributions, as the sound wave will be able to cross the fireball along its shortest direction. If this happens, and the amplitude of all three would be the same, then the magnitude of "nontriangular" harmonics (other than 3, 6, 9, . . .) drops further, as there is no need to cancel the nonexisting peak.

But why not observe the two-peak event shapes themselves? The reason is that there are multiple perturbations in any event, with random position in the transverse plane. The contribution of an individual fluctuation is very small, so that they can only be studied by finding statistically significant correlations of the particles. Remember that there is $\sim 10^9$ samples of available events with $\sim 10^3$ particles per events. Two-particle correlators use up to $\sim 10^6$ pairs of those in an event.

Say, if the elementary perturbation is local (δ function like in the transverse plane), then its angular position in the transverse plane is the only meaningful azimuthal orientation. The perturbations have random positions in the transverse plane, which we express as

$$\xi_n = \xi_p + \tilde{\xi}_n, \tag{4.3}$$

where the tilde indicates the angle relative to the perturbation and ξ_p is the random phase due to location of the perturbation.

As ξ_p is a random variable, all observables should be averaged over it.

What we want to show is that the way the correlations work out is quite different for (i) the two-body and (ii) the many-body (three or more) correlation functions. Indeed, in order to get the two-body correlation function one has to take a the square of the single-body distribution (4.2):

$$\sum_{n_1,n_2} v_{n_1} v_{n_2} \exp\left[i n_1\phi_1 + i n_2\phi_2 - i n_1\tilde{\xi}_{n_1} - i n_2\tilde{\xi}_{n_2} - i(n_1+n_2)\xi_p\right],$$

and average it over ξ_p randomly distributed over the circle. As a result, in the double sum above only the terms satisfying

$$n_1 + n_2 = 0 \tag{4.4}$$

survive. The double sum collapses into a single sum with the squared amplitude ϵ_n^2. Second, the sum becomes a function of the angular difference between the angles, $\Delta\phi = \phi_1 - \phi_2$, as expected from the symmetry. And, last but not least, all the phases ξ_n disappear. Therefore, two-particle correlators carry the same information as the "power spectrum" of the harmonics (we used the above for the example).

These facts are of course well known. The harmonics of the two-body correlator are

$$C_2(\Delta\phi) = \left\langle \frac{d^2N}{d\phi_1 d\phi_2} \right\rangle\Big|_{\xi_p}, \tag{4.5}$$

$$c_{n\Delta} = \frac{\int d(\Delta\phi) C_2(\Delta\phi)\cos(n\Delta\phi)}{\int d(\Delta\phi) C_2} = \langle v_n^2\rangle, \tag{4.6}$$

or squared amplitudes of the original harmonics, averaged over the events.

This is, for example, how Alver and Roland [17] and others have obtained their estimates for the "triangular" flow.

However, the situation is different for many-body (three or more) correlation functions. Indeed, if the single-body distribution (4.2) is cubed (or raised to higher power), one finds a triple sum in which random phases appear as $\exp[i(n_1 + n_2 + n_3)\psi_p]$, leading now to the "triangular" condition[2]

$$n_1 + n_2 + n_3 = 0. \tag{4.7}$$

Eliminating one of them (e.g., n_3) one finds the double sum

$$\sum_{n_1,n_2} v_{n_1} v_{n_2} v_{n_1+n_2} \exp\left\{i\left[n_1(\phi_1-\phi_3) + n_2(\phi_2-\phi_3) - n_1\left(\tilde{\xi}_{n_1} - \tilde{\xi}_{n_1+n_2}\right) - n_2\left(\tilde{\xi}_{n_1} - \tilde{\xi}_{n_1+n_2}\right)\right]\right\},$$

in which the relative phases of different harmonics are still present. Therefore one is still able to measure the relative phase of harmonics experimentally by focusing on the corresponding combinations:

$$\left\langle v_{n_1} v_{n_2} v_{n_3} \cos\left(n_1\xi_{n_1} + n_2\xi_{n_2} + n_3\xi_{n_3}\right)\right\rangle, \tag{4.8}$$

in which three integers must satisfy the condition (4.7). Obviously the number of solutions to condition (4.7) is larger than the number of harmonics, so all phases can be found. Experimentally, the price to pay is related to the smallness of the harmonics, which in such observables appear in the third (or higher) power. This makes it more difficult to measure, as the values extracted should be larger than the statistical noise.

It is at this point instructive to get back to our example of the two-peak distribution introduced above and see what those combinations of phase are in this case. One interesting solution to the condition (4.7) is $1 + 2 = 3$, which relates "enhanced" third harmonic with "subleading" 1 and 2. The sign of this average is defined by $\cos(\xi_1 + 2\xi_2 - 3\xi_3)$ and since, in our example $\xi_1 = \xi_2 = \pi$ and $\xi_3 = 0$, this combination of phases leads to $\cos(\xi_1 + 2\xi_2 - 3\xi_3) = -1$. But if one wants to measure the "enhanced" harmonics themselves, like in $3 + 3 = 6$, $6 + 3 = 9$, etc., the corresponding cosine would be close to 1 instead. Proceeding in this way one should be able to find such signs and conclude if the two-peak distributions are or are not close to reality.

Although hydro calculations is a subject of another paper, let us briefly discuss how comparison to theory should be done, assuming that the corresponding averages for some set of n_1, n_2, n_3 are experimentally measured. There are two steps to be done: First, using the (linearized) hydro one can approximate flow harmonics by the product of the initial deformations and the linear response terms

$$\left\langle v_{n_1} v_{n_2} v_{n_3} \cos\left(n_1\xi_{n_1} + n_2\xi_{n_2} + n_3\xi_{n_3}\right)\right\rangle = \left(\frac{v_{n_1}}{\epsilon_{n_1}}\right)\left(\frac{v_{n_2}}{\epsilon_{n_2}}\right)\left(\frac{v_{n_3}}{\epsilon_{n_3}}\right) \times \left\langle \epsilon_{n_1}\epsilon_{n_2}\epsilon_{n_3} \cos\left(n_1\xi_{n_1} + n_2\xi_{n_2} + n_3\xi_{n_3}\right)\right\rangle. \tag{4.9}$$

Second, one should change the flow angles we call ξ_n to the deformation angles ψ_n. One simple step is to phase shift [by (3.2)] the angle between flow and initial deformation. Note, however, that in each of the three terms, n_i in numerator and denominator cancel, leaving only 3π or simply the total sign change:

$$\cos\left(n_1\xi_{n_1} + n_2\xi_{n_2} + n_3\xi_{n_3}\right) = -\cos\left(n_1\psi_{n_1} + n_2\psi_{n_2} + n_3\psi_{n_3}\right). \tag{4.10}$$

The last step is to check for the direction (sign) of the flow. As we will see in Ref. [18], flow direction at freezeout oscillates as a function of n, so this sign should also be included in the phase. The resulting correlation of the amplitudes and orientations of the initial state fluctuations can be calculated from the initial state model, as we have done above for the first three harmonics resonance $1 + 2 = 3$ as well as $3 + 2 = 5$.

In fact it is not necessary to take Fourier moments of the correlation functions—it is sufficient to plot the correlation functions themselves. (This is especially useful if the experimental angular coverage in azimuth is incomplete.)

[2]Long after this paper had been posted we learned that a similar condition was proposed to be used to look for non-Gaussianity of the fluctuations of Cosmic Microwave Background (CMB) radiation. Our integers conjugated to azimuthal angle are then promoted to 2D angular momenta l_i on the sky, and so the condition means that three vectors can make a closed triangle. Thus the "triangular" name. To our knowledge, non-Gaussianity of the big bang has not yet been observed.

Defining the three-particle correlator as for the two-particle one, with the averaging over the perturbation angle

$$C_3(\phi_1,\phi_2,\phi_3)=\left\langle \frac{d^2N}{d\phi_1 d\phi_2 d\phi_3}\right\rangle_{\psi_p}, \tag{4.11}$$

one finds it, for central collisions, to be a function of the two angle differences, say $\phi_1-\phi_3$ and $\phi_2-\phi_3$. The corresponding 2D plots for the two- and three-peak distributions look quite different and should be relatively easy to separate.

B. Mid-central collisions and two-body correlators relative to event plane

A nonzero impact parameter violates axial symmetry and creates "directed flows," for example, the famous elliptic flow with $\langle v_2\rangle\neq 0$. By mid-central collisions we mean a centrality region in which $\langle\epsilon_2\rangle$ is large itself and is also large compared to its fluctuations (recall that it is not so for central and very peripheral collisions). For example, ϵ_2 is 0.5 (0.3) for $N_p=$ 100 (200) participants, with $\delta\epsilon_2\approx 0.1$. Furthermore, as seen in Fig. 4(b), its angle ψ_2 is very much directed at $\pm\pi/2$ (the tips of the almond) and therefore [using Eq. (3.2) for $n=2$] the flow angle is peaked "in-plane," and $\xi_2=0,\ \pi$, as indeed is observed.

If so, for one of the harmonics being the second (e.g., $n_3=\pm 2$) one can approximate a product of three deformations as follows:

$$\begin{aligned}&\left\langle v_{n_1}v_{n_2}v_{n_3}\cos\left(n_1\xi_{n_1}+n_2\xi_{n_2}+n_3\xi_{n_3}\right)\right\rangle\\ &\quad\approx\left(\frac{v_{n_1}}{\epsilon_{n_1}}\right)\left(\frac{v_{n_2}}{\epsilon_{n_2}}\right)\left(\frac{v_2}{\epsilon_2}\right)\langle\epsilon_2\rangle\left\langle\epsilon_{n_1}\epsilon_{n_2}\cos\left(n_1\xi_{n_1}+n_2\xi_{n_2}\right)\right\rangle,\end{aligned} \tag{4.12}$$

by factoring out large and nonfluctuating $\langle\epsilon_2\rangle$ from the two other harmonics which are small and fluctuating. Note that the resonance condition now means $n_1\pm 2=n_2$, and that, by putting $\xi_2=0$, we have selected a frame in which the (experimentally determined reaction plane) is the x axis.

Basically the lesson here is that, for mid-central collisions, the "reaction plane" plays the same role as the third body, so we are reduced to two small fluctuating and correlated harmonics. The simplest nontrivial example of the resonance condition of this kind is $3-1-2=0$ (recently studied by Teaney and Yan [35]), while the next is $5-3-2=0$.

We had already calculated the combinations of two fluctuating harmonics with the appropriate cosines above, for these two cases, in the Glauber model. They are by no means small. For example, for the centrality bin with [100. . . 300] participants, they are

$$\langle\epsilon_1\epsilon_3\cos(3\psi_3-\psi_1)\rangle\sim -0.015, \tag{4.13}$$

$$\langle\epsilon_3\epsilon_5\cos(3\psi_3-5\psi_5)\rangle\sim -0.05, \tag{4.14}$$

and therefore we expect it to be observable, with about as large statistics as needed for the usual quadratic fluctuations.

V. SUMMARY

In this work we have (i) discussed the setting, identifying the main scales of the problem. Then (ii) we studied in detail the initial state fluctuations originating from nucleon positions, emphasizing existence of the nontrivial phase relations between different harmonics. Finally, (iii) we discussed correlation functions of two and many hadrons and pointed out the principal difference between them, with the latter allowing us to measure experimentally the relative phases of these harmonics.

Let us now recapitulate the lessons from this study in a bit more detail.

Unfortunately, the perturbations we speak about are too small to be measured directly on an event-by-event basis and should be instead reconstructed from the statistically obtained correlation functions. One good thing coming from it is that many independent fluctuations from local perturbations in a single event and in the ensemble are treated by correlation functions, in which all trivial uncorrelated effects are statistically subtracted and absent.

Traditionally, the initial state perturbations and final state corrections to collective flow are considered in a form of their angular harmonics, which we call ϵ_n and v_n, respectively. Their relation is calculated by the hydrodynamics—the details of which (in the linearized form) is the subject of our companion paper [18].

Most papers on the subject consider ϵ_n and v_n as independent random variables, which are incoherent fluctuations, added in quadratures and ignore their phases ξ_n and ψ_n, respectively. We, however, pointed out that, while this can be done for the two-particle correlations, it is not so in general. Correlators of many-particle (three and more) correlations include those phases (as do two-body correlations) relative to event plane for mid-central collisions. Many different "triplets" n_1, n_2, n_3 related by the "triangular condition" between them can be measured, providing experimental opportunity to find out if and how the perturbations are correlated. This needs to be done to refine models of the initial state. The magnitude of a few such terms we have estimated in the Glauber model, and they are comparable in magnitude to the terms already studied. We also presented theoretical toy models, in which phases between harmonics are especially simple.

Coherence in phases of the deformations imply interferences between the harmonics of the flow. Only by adding them together can one follow how small "hot" (or "cold") spots created by quantum fluctuations of interacting nucleons propagate away from the point of origin. Only in this way can one understand the role played by the "hydrodynamical causality," insisting that a large part of the fireball should remain completely unaffected by the perturbation since the signal cannot possibly reach it before the freezeout. Only a complete Green function, collecting all hydro harmonics, describes these shapes of propagating waves, as we detail in Ref. [18].

There are two basic scales defining those perturbations: the sound horizon H_s (2.2) and the "the viscous horizon scale" R_v (2.6). The former gives the size of the perturbation,

stemming from a local perturbation; the latter gives its width. We have, for example, argued that, by changing the centrality of the collisions, one can change the relation between the (smaller) fireball size and the sound horizon: this should dramatically change the shape of the event (see Fig. 4 for explanation).

It is an important objective of the experimental heavy-ion program in general to measure these two scales, extracting experimental values of the speed of sound and viscosity. One specific idea proposed in this work is that, by changing centrality, one can locate the transition when H_s and the smaller size of the overlap region are equal, observing the change of shape of the underlying event, from those with two peaks to three-peaks ones. If found, it would be a very spectacular confirmation of the view that sound waves can travel large distances $\sim R$ during heavy-ion collisions. It will also put to rest various models which assume significantly shorter freezeout time than that predicted by hydrodynamics.

ACKNOWLEDGMENTS

This work was supported in part by US-DOE Grant No. DE-FG-88ER40388. Discussion with Frederique Grassi, explaining their finding in detail, have been very helpful. We also benefited from multiple discussion with Derek Teaney.

[1] J. Adams *et al.* (STAR Collaboration), Nucl. Phys. A **757**, 102 (2005).
[2] K. Adcox *et al.* (PHENIX Collaboration), Nucl. Phys. A **757**, 184 (2005).
[3] I. Arsene *et al.* (BRAHMS Collaboration), Nucl. Phys. A **757**, 1 (2005).
[4] B. B. Back *et al.*, Nucl. Phys. A **757**, 28 (2005).
[5] D. Teaney, J. Lauret, and E. V. Shuryak, Phys. Rev. Lett. **86**, 4783 (2001).
[6] T. Hirano, Acta Phys. Pol. B **36**, 187 (2005).
[7] C. Nonaka and S. A. Bass, Phys. Rev. C **75**, 014902 (2007).
[8] S. A. Bass and A. Dumitru, Phys. Rev. C **61**, 064909 (2000).
[9] K. Aamodt *et al.* (ALICE Collaboration), Phys. Rev. Lett. **105**, 252302 (2010).
[10] E. Shuryak, Physics **3**, 105 (2010).
[11] P. Romatschke and U. Romatschke, Phys. Rev. Lett. **99**, 172301 (2007).
[12] K. Dusling and D. Teaney, Phys. Rev. C **77**, 034905 (2008).
[13] U. Heinz and H. Song, J. Phys. G **35**, 104126 (2008).
[14] G. Aad *et al.* (ATLAS Collaboration), Phys. Rev. Lett. **105**, 252303 (2010).
[15] J. Casalderrey-Solana, E. V. Shuryak, and D. Teaney, J. Phys. Conf. Ser. **27**, 22 (2005); Nucl. Phys. A **774**, 577 (2006); L. M. Satarov, H. Stoecker, and I. N. Mishustin, Phys. Lett. B **627**, 64 (2005).
[16] S. Mrowczynski and E. V. Shuryak, Acta Phys. Pol. B **34**, 4241 (2003).
[17] B. Alver and G. Roland, Phys. Rev. C **81**, 054905 (2010).
[18] P. Staig and E. Shuryak, arXiv:1105.0676.
[19] J. Casalderrey-Solana and E. V. Shuryak, arXiv:hep-ph/0511263.
[20] E. Shuryak, Phys. Rev. C **80**, 054908 (2009); **80**, 069902 (2009).
[21] R. Andrade, F. Grassi, Y. Hama, and W. L. Qian, J. Phys. G **37**, 094043 (2010).
[22] J. Takahashi *et al.*, arXiv:0902.4870, and references therein.
[23] K. Werner, I. Karpenko, T. Pierog, M. Bleicher, and K. Mikhailov, arXiv:1004.0805.
[24] G. -Y. Qin, H. Petersen, S. A. Bass, and B. Muller, Phys. Rev. C **82**, 064903 (2010).
[25] R. A. Sunyaev and Y. B. Zeldovich, Annu. Rev. Astron. Astrophys. **18**, 537 (1980).
[26] M. Lublinsky and E. Shuryak, Phys. Rev. D **80**, 065026 (2009).
[27] M. P. Heller, R. A. Janik, and P. Witaszczyk, arXiv:1103.3452.
[28] G. Baym, B. Blattel, L. L. Frankfurt, H. Heiselberg, and M. Strikman, Phys. Rev. C **52**, 1604 (1995).
[29] L. D. McLerran and R. Venugopalan, Phys. Rev. D **49**, 2233 (1994).
[30] H. Kowalski and D. Teaney, Phys. Rev. D **68**, 114005 (2003).
[31] D. M. Ostrovsky, G. W. Carter, and E. V. Shuryak, Phys. Rev. D **66**, 036004 (2002).
[32] D. Kharzeev and A. Zhitnitsky, Nucl. Phys. A **797**, 67 (2007).
[33] T. S. Biro, H. B. Nielsen, and J. Knoll, Nucl. Phys. B **245**, 449 (1984).
[34] H. Sorge, M. Berenguer, H. Stoecker, and W. Greiner, Phys. Lett. B **289**, 6 (1992).
[35] D. Teaney and L. Yan, Phys. Rev. C **83**, 064904 (2011).